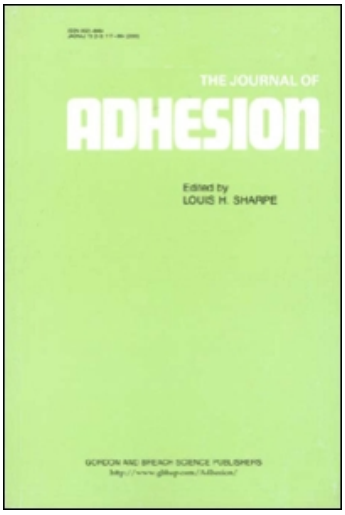

The Journal of Adhesion
Publication details, including instructions for authors and subscription information:
http://www.informaworld.com/smpp/title~content=t713453635

Effects of bond parameters on fatigue characteristics of a cocured double lap joint subjected to cyclic tensile loads

Kum Cheol Shin[a]; Jung Ju Lee[a]
[a] Department of Mechanical Engineering, Korea Advanced Institute of Science and Technology, Daejeon, Korea

Online publication date: 08 September 2010

To cite this Article Shin, Kum Cheol and Lee, Jung Ju(2003) 'Effects of bond parameters on fatigue characteristics of a cocured double lap joint subjected to cyclic tensile loads', The Journal of Adhesion, 79: 6, 581 — 596
To link to this Article: DOI: 10.1080/00218460309542
URL: http://dx.doi.org/10.1080/00218460309542

The Journal of Adhesion, 79: 581–596, 2003

ISSN: 0021-8464
DOI: 10.1080/00218460390201338

Taylor & Francis
Taylor & Francis Group

EFFECTS OF BOND PARAMETERS ON FATIGUE CHARACTERISTICS OF A COCURED DOUBLE LAP JOINT SUBJECTED TO CYCLIC TENSILE LOADS

Kum Cheol Shin
Jung Ju Lee
Department of Mechanical Engineering,
Korea Advanced Institute of Science and Technology,
Kusong-dong, Yusong-gu, Daejeon, Korea

A cocured joint whose manufacturing process is simpler than that of an adhesively bonded joint is attractive for composite structures due to its several benefits. Fatigue behavior in the cocured joint is important because under alternating loads it will fail at stress levels much lower than it can withstand under monotonic loading. Although some researchers have recently reported on cocured joints, there are only a few articles published on the fatigue characteristics of cocured joints.

In this article, effects of bond parameters on fatigue characteristics of a steel-composite cocured double lap joint under cyclic tensile loads were experimentally investigated. In order to observe stress distributions near the interface edge of the cocured double lap joint, finite element analysis was also performed. We considered the surface roughness of the steel adherend and the stacking sequence of the composite adherend as bond parameters. A fatigue failure mechanism of the cocured double lap joint was explained systematically by investigating the surfaces of failed specimens and stress distributions at the interface edge. Failure criteria of the cocured double lap joint under cyclic tensile loads were shown graphically.

Keywords: Cocured double lap joint; Fatigue characteristics; Surface roughness; Stacking sequence

INTRODUCTION

Fatigue is the phenomenon of failure or fracture of a material, joint, or structure under repeated or oscillatory loading. Fatigue

Received 20 June 2002; in final form 8 October 2002.

Address correspondence to Jung Ju Lee, Department of Mechanical Engineering, Korea Advanced Institute of Science and Technology, 373-I, Kusong-dong, Yusong-gu, Daejeon 305-701, Korea. E-mail: jjlee@mail.kaist.ac.kr

behavior in joint structures is important because under alternating loads joints will fail at stress levels much lower than they can withstand under monotonic loading. Adhesive joints are generally regarded as possessing good fatigue properties compared with mechanical joints due to the relatively more even stress distribution in the joint [1].

The use of a cocured joining method for composite structures is attractive because of several benefits [2]. A cocured joint is composed of two adherends including the composite adherend, where the excess resin extracted from the composite adherend during the curing process accomplishes the cocured joining process. The cocured joining method, whose curing and bonding processes are simultaneously achieved, can be regarded as an adhesive joining method because it uses excess resin extracted from the composite adherend as an adhesive. Therefore, the manufacturing process of the cocured joint is simpler than that of an adhesively bonded joint, which uses an additional adhesive for the bonding process [3].

Comparing some research on the adhesively-bonded joint composed of steel and composite adherends with that on the cocured joint under static tensile loads, the bond strength of the cocured joint is as good as that of the adhesively bonded joint [3–5]. However, since the design stress level in cyclic loads is often smaller than the joint strength obtained from the static tensile load test, it is important to establish proper fatigue design criteria. Although some researchers have reported on cocured joints [2–3, 6–12], there are only a few papers published on the fatigue characteristics of cocured joints [13].

The joint strength of a lap joint is affected by the surface roughness of both adherends [14–17]. When joining different adherends, such as a composite adherend to a metal adherend, significant out-of-plane stresses may occur due to the difference in stiffness between the two adherends [18–19]. In addition, since the composite adherend shows different stiffness with respect to the stacking sequence, it is important to consider the dependence of the fatigue strength of the cocured lap joint on the stacking sequence of the composite adherend.

In this paper, the fatigue strength of a cocured double lap joint with steel and carbon fiber-epoxy composite adherends subjected to cyclic tensile loads was investigated experimentally with respect to two bond parameters, namely the surface roughness of the steel adherend and the stacking sequence of the composite adherend. The effects of the bond parameters on the fatigue characteristics of the cocured double lap joint were explained systematically.

SPECIMEN FABRICATION AND EXPERIMENTAL PROCEDURE

In order to improve the joint strength of the cocured joint, surface treatment of the steel adherend should be carefully performed using various sandpapers. The composite adherend, which is the other adherend of the joint, is stacked with composite prepregs. Then, the composite adherend is lightly prebonded to the steel adherend before curing so that it does not shift during curing. An uncured cocured joint is completely cured under 0.7 MPa pressure, using the manufacturer's recommended cure cycle in the autoclave. Figure 1 shows the cure cycle for a carbon fiber-epoxy composite material. Since the excess resin plays the role of an adhesive, the cocured joint should be cured without a resin bleeder and peel ply to prevent the excess resin from bleeding [7, 20].

After the curing and bonding processes, the cocured joint should be finished using various abrasive sandpapers to obtain consistent joint strength by eliminating sharp edges. A complete cocured joint is composed of two adherends and a resin layer with about 10 μm thickness. Figure 2 shows a cocured double lap joint specimen, which was selected on the basis of ASTM D3528 [21]. A Teflon block surrounded by steel and composite adherends was used to prevent the two steel adherends from bonding to each other. Table 1 shows the properties of the carbon fiber-epoxy composite. Specimens selected in this paper were of three types: A-type with $[0]_{16T}$ stacking sequence

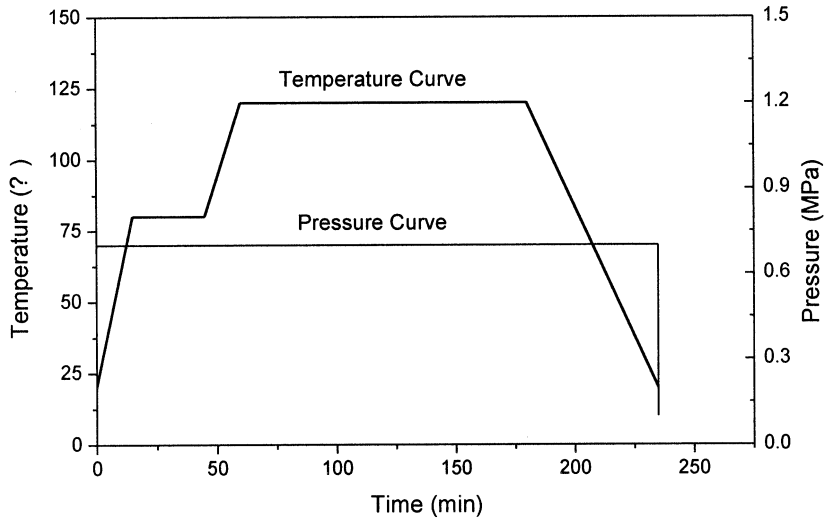

FIGURE 1 Cure cycle for the carbon fiber-epoxy composite.

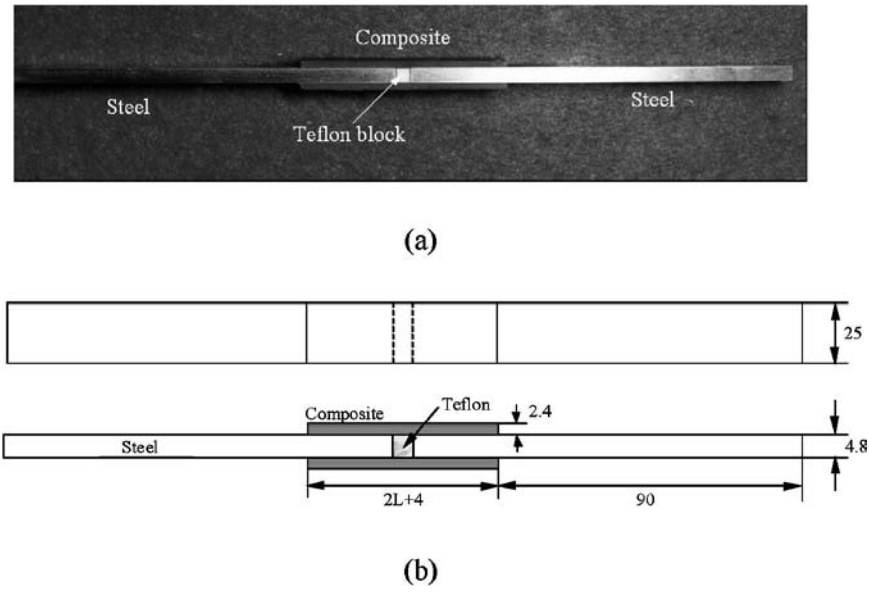

FIGURE 2 A cocured double lap joint specimen. (a) Photograph of the specimen and (b) shape and dimensions of the specimen.

and 1.2 μm surface roughness, B-type with $[0]_{16T}$ stacking sequence and 0.3 μm surface roughness, and C-type with $[\pm 45]_{4S}$ stacking sequence and 1.2 μm surface roughness. Bond length of the cocured double lap joint specimen was 20 mm.

The cocured double lap joint specimens were tested using a 250 kN materials testing system (MTS, Systems Corp.,

TABLE 1 Material Properties of the Unidirectional Carbon Fiber-Epoxy Composite

E_L(GPa)	130
E_T(GPa)	8
G_{LT}(GPa)	6
ν_{LT}	0.28
X^t(MPa)	1800
Y^t(MPa)	50
S (MPa)	75
Ply Thickness (mm)	0.15
Density (g/cm^3)	1.56

E_L, longitudinal tensile modulus; E_T, transverse tensile modulus; G_{LT}, shear modulus; ν_{LT}, Poisson's ratio; X^t, longitudinal tensile strength; Y^t, transverse tensile strength; S, shear strength.

Minneapolis, Minnesota, USA). Cyclic tensile tests were performed under the condition of load ratio $R = 0.1$ and a loading frequency of $f = 5$ Hz. Cyclic tensile loads applied to the cocured double lap joint specimens were 30%, 40%, 50%, 60%, and 70% of their static tensile load bearing capacities. The following relationships and definitions are used when discussing mean and alternating loads.

$R = \frac{P_{\min}}{P_{\max}} =$ load ratio
$\Delta P = P_{\max} - P_{\min} =$ load range
$P_{\max} =$ maximum load
$P_{\min} =$ minimum load
$P_S =$ static tensile load-bearing capacity

EXPERIMENTAL RESULTS AND DISCUSSION

Figure 3 shows typical failure surfaces of the steel adherend of the cocured double lap joint with the A-type condition, which were obtained from cyclic tensile test specimens. The adhesive area was torn apart from the composite adherend. The amount of the adhesive area attached to the steel adherend could be considered to be related to

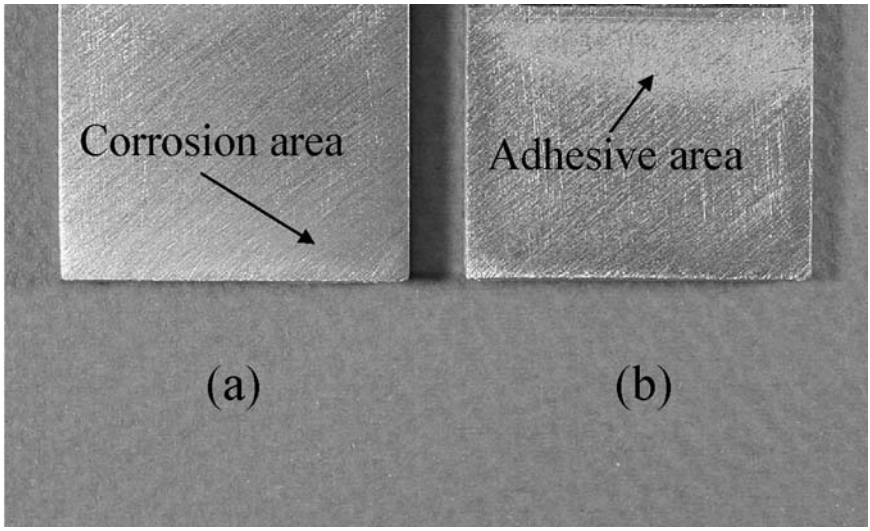

FIGURE 3 Photograph of the typical failure surfaces of the steel adherend obtained from the failed cyclic tensile test specimens. The specimens have $[0]_{16T}$ stacking sequence and 1.2 μm surface roughness. (a) $P_{\max} = 0.5P_S$, (b) $P_{\max} = 0.7P_S$.

the joint strength of the cocured double lap joint. In the case of the A-type specimen the adhesive area attached to the steel adherend is thick and large. Initial failure at the interface between steel and composite adherends starts at the edge of the bonded area near the Teflon block, because stress concentration occurs at the edge of the bonded area. As the tensile load is repeatedly applied to the cocured joint after initial failure, the failure mechanism changes to cohesive failure in the thin adhesive layer. Therefore, the failure mechanism of the cocured double lap joint with the A-type condition under cyclic tensile loads is a partial cohesive failure in the thin resin layer.

In order to analyze the failure mechanism of the cocured double lap joint subjected to a tensile load and a thermal load, the stress distributions were analyzed using ABAQUS 5.8, which is a commercial finite element analysis software [22]. The cocured double lap joint was modeled as a three-dimensional solid structure. Since the average thickness of the thin resin layer between the adherend surfaces was about 15 μm, the resin layer was ignored in this finite element analysis. Therefore, the cocured double lap joint was assumed as perfectly bonded at the interface between the steel adherend and the composite laminate. The Teflon block between the adherends was ignored in this analysis because of its low modulus (0.6 GPa) and slippery, nonbonding surface. Since the cocured double lap joint was a quarterly symmetric configuration, only a quarter of the cocured double lap joint was modeled. Figure 4 shows the quarterly symmetric configuration and finite element meshes of the cocured double lap joint. The element used for the steel adherend was a 20-node, three-dimensional isotropic solid element, and the element used for the composite adherend was a 20-node, three-dimensional orthotropic solid element. Figure 5 shows the coordinate system of the cocured double lap joint for the finite element analysis.

In the case of $P_{\max} = 0.5P_S$, the cyclic load applied to the specimen is not large and the number of cycles to failure ($N_f = 108,786$) is large. The adhesive area attached to the steel adherend is not large. This is caused by the stable failure mechanism of the cocured double lap joint under the low cyclic load. A corrosion area on the steel adherend in

FIGURE 4 Finite element model for the cocured double lap joint.

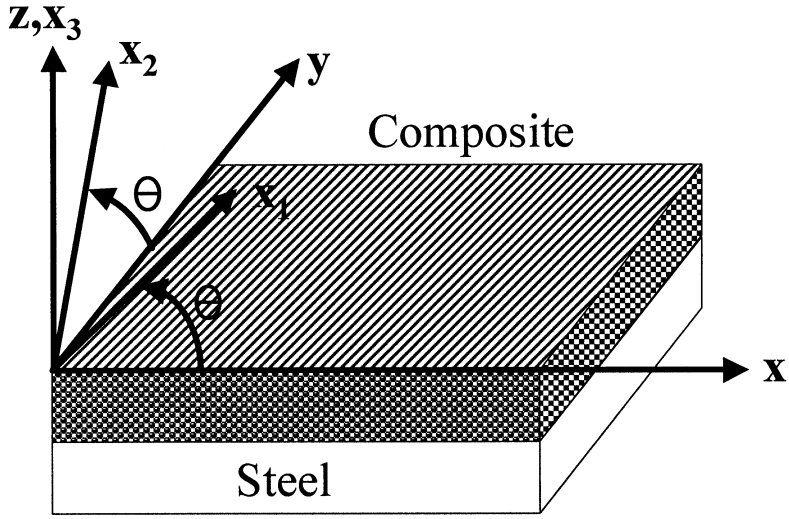

FIGURE 5 Coordinate system of the cocured double lap.

Figure 3a occurs due to interfacial transverse compressive stress, repeated load, and the relative motion in the interface. This type of corrosion occurs at contact areas between materials under loads subjected to vibration and slip [23]. The basic requirements for this type of corrosion are as follows: the interface must be under load, vibration or repeated relative motion of the two materials must occur, and the load and the relative motion of the interface must be sufficient to produce slip or deformation on the surfaces. In this case, the A-type specimen meets these three basic requirements.

Figure 6 shows interfacial transverse stress distributions at the interface of the cocured double lap joint with A-type condition. In Figure 6a, interfacial transverse normal stress is compressive at $x = 0$. In general, it is known that the interfacial transverse compressive stress does not affect the crack growth. However, in this case the interfacial transverse compressive stress affects the occurrence of the corrosion between the steel and composite adherends under the cyclic tensile loads. In the case of $P_{\max} = 0.7P_S$, however, the cyclic load applied to the specimen is large and the number of cycles to failure ($N_f = 13,445$) is small. There is large adhesive area attached to the steel adherend because the co-cured double lap joint is under a large cyclic load which can induce unstable failure of the joint. There is no corrosion area on the failure surface of the steel adherend because the cyclic load applied to the specimen is too large for the corrosion to occur at the interface and the relative deformation is too small. In

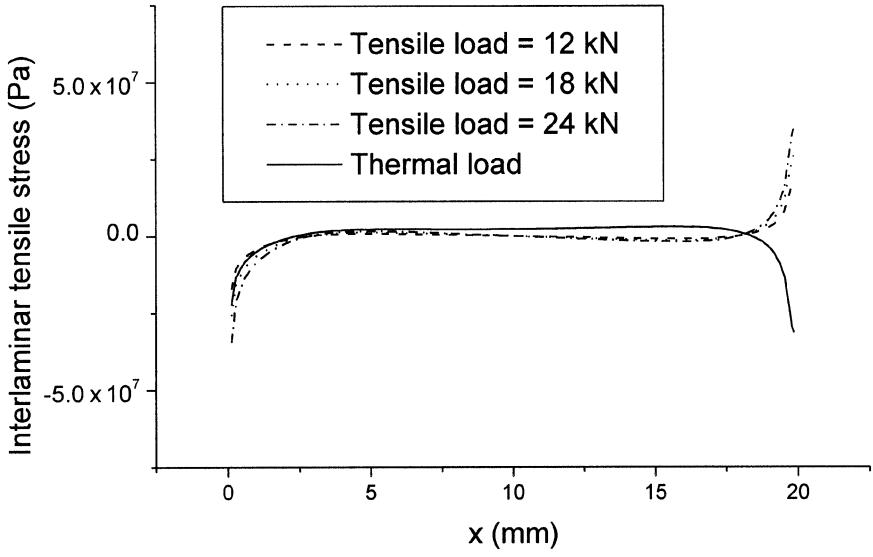

(a)

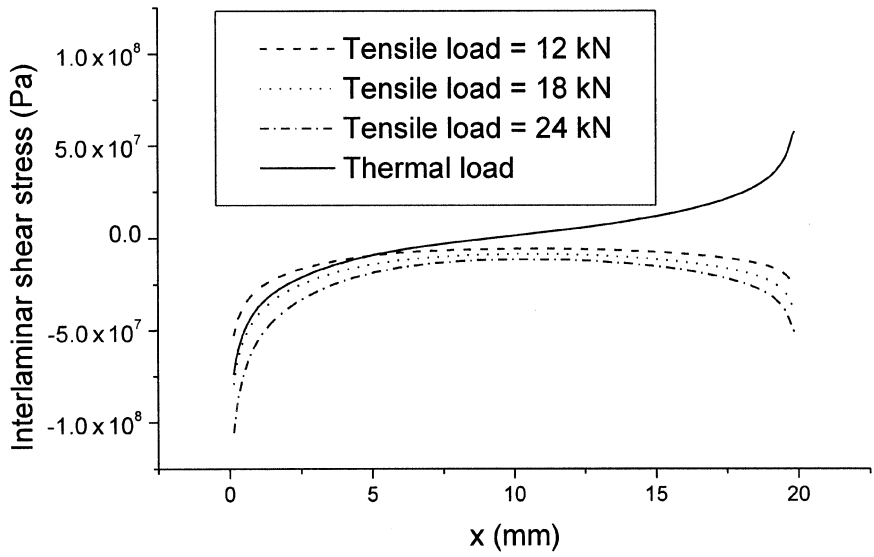

(b)

FIGURE 6 Interfacial transverse stress distributions at the interface of the cocured double lap joint with A-type condition. (a) Interfacial transverse normal stress distribution; (b) interfacial transverse shear stress distribution.

Figure 6b, the interfacial transverse shear stress near the Teflon block is large enough to induce the failure of the cocured double lap joint. Therefore, it is important to consider the interfacial transverse shear stress in designing the cocured double lap joint with the A-type specimen (or B-type specimen).

Figure 7 shows typical failure surfaces of the steel adherend of the cocured double lap joint with the B-type condition, which were also obtained from cyclic tensile test specimens. The adhesive area, which is related to the joint quality between the two adherends, is not as thick as the A-type specimen's adhesive area. This means that the B-type joint specimens possibly might not have as good joint strength as the A-type joint specimens do, although their adhesive area is large. Therefore, surface roughness of the steel adherend of the cocured double lap joint can affect the joint strength. The failure mechanism is similar to the A-type specimen. As the cyclic tensile load is repeatedly applied to the specimen, the interfacial failure mode is changed to the cohesive failure mode in the thin adhesive layer. In the case of $P_{\max} = 0.5P_S$, the cyclic load applied to the specimen is not large and the number of cycles to failure ($N_f = 236,674$) is large. The adhesive area attached to the steel adherend is caused by the stable failure

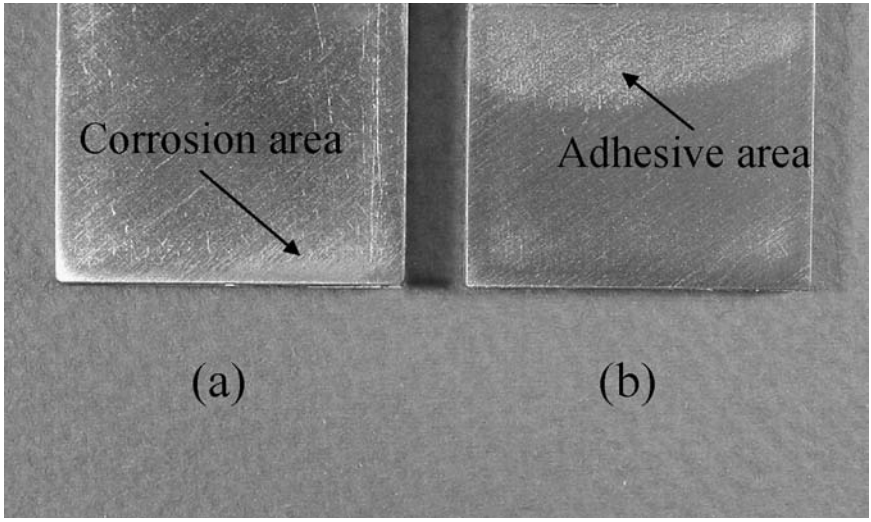

FIGURE 7 Photograph of the typical failure surfaces of the steel adherend obtained from the failed cyclic tensile test specimens. The specimens have $[0]_{16T}$ stacking sequence and 0.3 μm surface roughness. (a) $P_{\max} = 0.5P_S$, (b) $P_{\max} = 0.7P_S$.

mechanism of the cocured double lap joint under the low cyclic load. The corrosion area on the steel adherend is not as thick as the A-type specimen's corrosion area because surface roughness is not large. In the case of $P_{\max} = 0.7P_S$, the cyclic load applied to the specimen is large and the number of cycles to failure ($N_f = 13{,}902$) is small. From this investigation, we can conclude that surface roughness, which resists fatigue crack propagation, affects fatigue characteristics of the cocured double lap joint.

Figure 8 shows typical failure surfaces of the steel adherend of the cocured double lap joint with the C-type condition, obtained from cyclic tensile test specimens. The adhesive area attached to the steel adherend is not thick. This means, possibly, that the joint might not have good joint strength. However, the corrosion area on the steel adherend is thick because compressive stress in the joint is very large. The corrosion area on the steel adherend of the C-type specimen subjected to low cyclic load is largest among all kinds of specimens. Figure 9 shows interfacial transverse stress distributions in the cocured double lap joint with the C-type condition. In Figure 9a, interfacial transverse compressive stress in the joint is larger than for A- and B-type specimens. This large compressive stress increases the

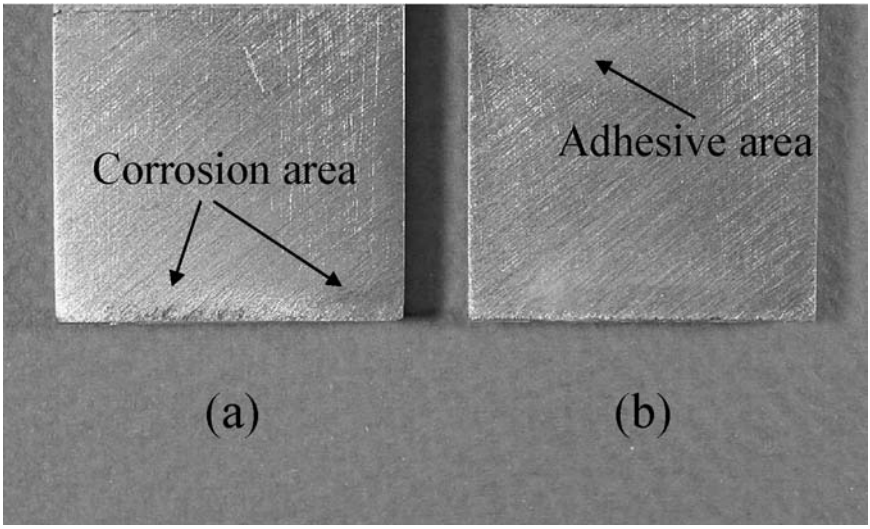

FIGURE 8 Photograph of the typical failure surfaces of the steel adherend obtained from the failed cyclic tensile test specimens. The specimens have $[\pm 45]_{4S}$ stacking sequence and 1.2 μm surface roughness. (a) $P_{\max} = 0.5P_S$, (b) $P_{\max} = 0.7P_S$.

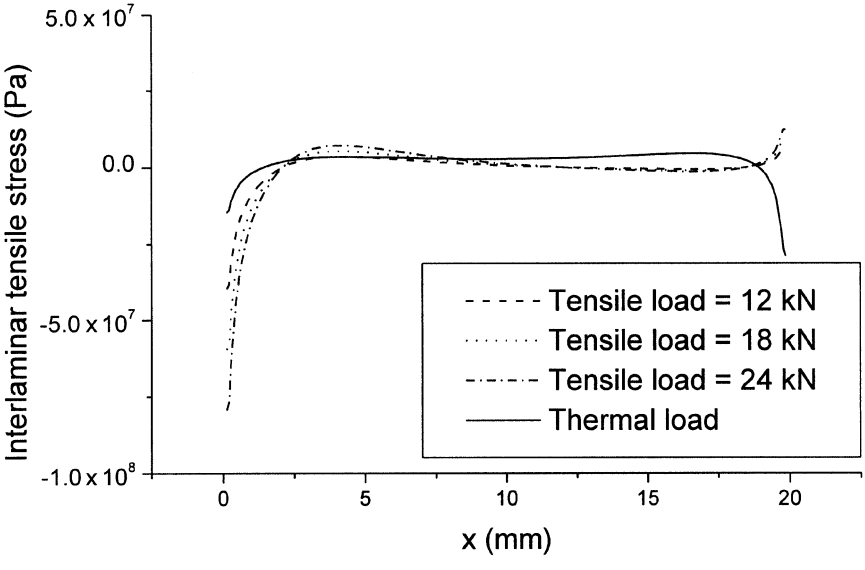

(a)

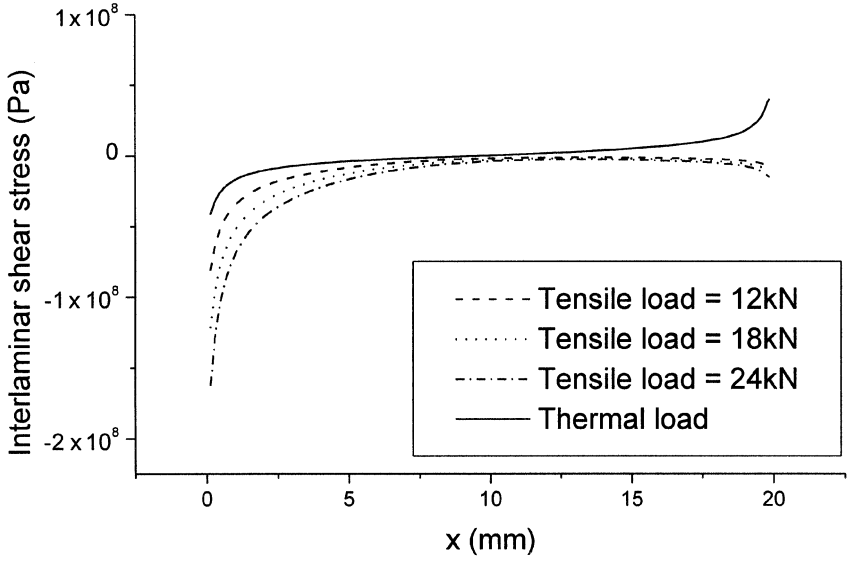

(b)

FIGURE 9 Interfacial transverse stress distributions at the interface of the cocured double lap joint with C-type condition. (a) Interfacial transverse normal stress distribution, (b) interfacial transverse shear stress distribution.

occurrence of the corrosion between the steel and composite adherends under the cyclic tensile loads. In the case of $P_{\max} = 0.5P_S$, the cyclic load applied to the specimen is not large and the number of cycles to failure ($N_f = 431{,}023$) is large. In the case of $P_{\max} = 0.7P_S$, however, the cyclic load applied to the specimen is large and the number of cycles to failure ($N_f = 10{,}690$) is small. There is a large adhesive area attached to the steel adherend because the cocured double lap joint is under a large cyclic load. In Figure 9b, the interfacial transverse shear stress near the Teflon block is large enough to induce the failure of the cocured double lap joint. Therefore, it is important to consider the interfacial transverse shear stress in designing the cocured double lap joint with the C-type specimen.

Figure 10 shows the relationship between the maximum load and the number of cycles to failure of the cocured double lap joint obtained from cyclic tensile tests. The A-type specimens, which have $[0]_{16T}$ stacking sequence and 1.2 μm surface roughness, have better fatigue resistance than the B-type specimens with $[0]_{16T}$ stacking sequence and 0.3 μm surface roughness when considering experimental results under the same cyclic load levels. This result is caused by the difference of the surface roughness, which often determines the size of the

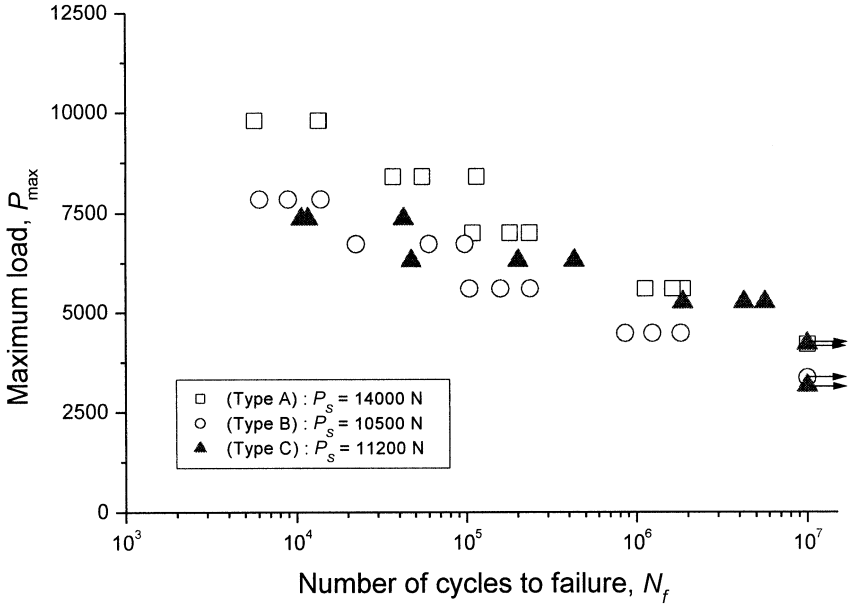

FIGURE 10 Relationship between the maximum load and the number of cycles to failure of the cocured double lap joint.

contact area between the two adherends. The A-type specimen has a little more contact area than the B-type specimen.

The C-type specimens, which have $[\pm 45]_{4S}$ stacking sequence and 1.2 μm surface roughness, have worse fatigue resistance than the A-type specimens at the high cyclic load level when considering experimental results under the same cyclic load levels. However, the C-type specimens have as good fatigue resistance as the A-type specimens at the low cyclic load level. This result is caused by the transverse stress distribution in the cocured double lap joint with C-type condition, which has larger transverse shear stress than that with the A-type condition at the large applied tensile load and about the same transverse shear stress as the A-type specimens at the low applied tensile load. Therefore, it would be better to consider first the stacking sequence of the composite adherend of the cocured double lap joint using stress distributions obtained from the finite element analysis and then to select the optimum surface roughness of the steel adherend.

Figure 11 shows the relationship between the normalized load range and the number of cycles to failure of the cocured double lap joint

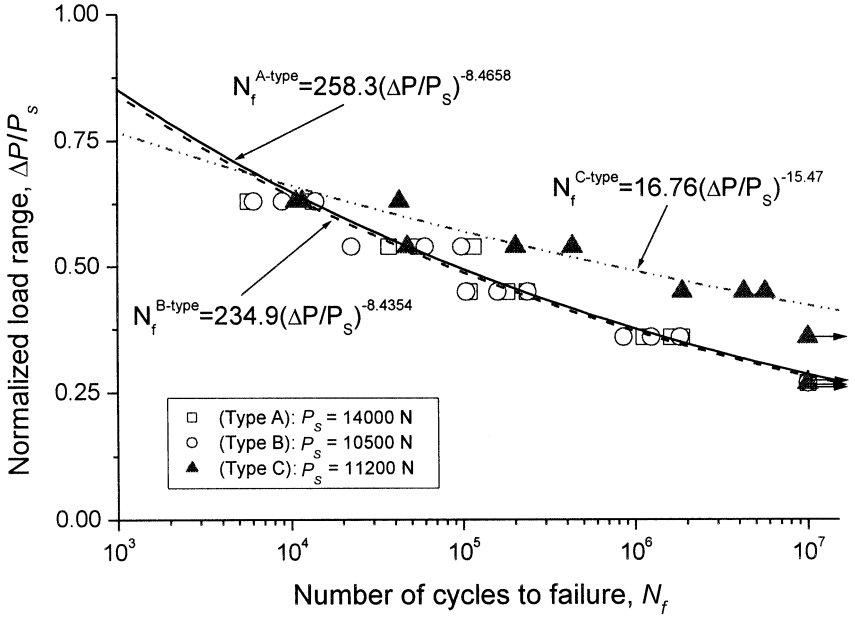

FIGURE 11 Relationship between the normalized load range and the number of cycles to failure of the cocured double lap joint.

obtained from cyclic tensile tests. Scattered data in Figure 11 were obtained from the experiments, and the three curves through the data represent power law relationships between the normalized load range and the fatigue failure life. The typical form of the relationship is:

$$N_f = A\left(\frac{\Delta P}{P_S}\right)^n,$$

where A and n are constants which should be determined from scattered data using the least-squares approximation [24]. The curves fitting the experimental data from the three types of joints were determined by calculating A and n. The constants A and n for the three types of joints are shown in Figure 11. Investigating the fitting curves obtained by considering the power law, the A-type joint specimens have about the same fatigue characteristics as the B-type joint specimens. This is caused by the fact that we considered the normalized load range, which is based on the static tensile load-bearing capacity of the joint, as the applied load. Therefore, we can characterize the fatigue resistance of the cocured double lap joint with different surface roughness by observing the static fatigue resistance. This means that we should also consider the magnitude of the static tensile load-bearing capacity, P_S, of the joint because these results are based on the cyclic load range. The A- and B-type joint specimens have good fatigue characteristics in the high cyclic tensile load range. The C-type joint specimens have better fatigue characteristics than A- and B-type joint specimens in the overall applied cyclic load range except for the very high applied cyclic load range.

CONCLUSIONS

In this work, fatigue characteristics of the cocured double lap joint were experimentally investigated with respect to several bond parameters. From the experimental investigations, the following conclusions were derived:

1. The failure mechanism of the cocured double lap joints with A-, B-, and C-type conditions under cyclic tensile load was a partial cohesive failure in the thin adhesive layer. Interfacial transverse shear stress was the most important component affecting the failure of the cocured double lap joints. Because stress concentration occurred at the edge of the bonded area, failure started at the interface in the interfacial failure mode. As the cyclic tensile load was repeatedly applied to the specimen, the

interfacial failure mode changed to the cohesive failure mode in the thin adhesive layer.

2. The adhesive area on the steel adherend of the cocured double lap joint under the low cyclic load was not large. This was caused by the stable failure mechanism of the cocured double lap joint under the low cyclic load. The corrosion area at the interface between the two adherends appeared on the steel adherend of the cocured double lap joint under the low cyclic load. The corrosion area on the steel adherend of the C-type specimen subjected to low cyclic load was the largest among all kinds of specimens. In the case of the cocured double lap joint under the high cyclic load, there was a large adhesive area which meant change of the failure mode from interfacial failure to cohesive failure.
3. Surface roughness of the steel adherend and stacking sequence of the composite adherend were important bond parameters affecting joint strength. It would be better to consider first the stacking sequence of the composite adherend of the cocured double lap joint using stress distributions obtained from the finite element analysis and then to select the optimum surface roughness of the steel adherend.
4. The A- and B-type joint specimens had good fatigue characteristics in the high cyclic tensile load range. The C-type joint specimens had better fatigue characteristics than the A- and B-type joint specimens under the overall applied cyclic load range except for the high applied cyclic load range. We could characterize the fatigue resistance of the cocured double lap joint with different surface roughness by observing the static fatigue resistance. This means that we should also consider the magnitude of the static tensile load-bearing capacity, P_S, of the joint because these results are based on the cyclic load range.

REFERENCES

[1] Kinloch, A. J., *Adhesion and Adhesives: Science and Technology* (Chapman and Hall, London, 1987), pp. 339–350.
[2] Shin, K. C., and Lee, J. J., *J. Adhesion Sci. Tech.* **14**, 1539–1556 (2000).
[3] Shin, K. C., Lee, J. J., and Lee, D. G., *J. Adhesion Sci. Tech.* **14**, 123–139 (2000).
[4] Choi, J. K., and Lee, D. G., *J. Adhesion* **48**, 235–250 (1995).
[5] Jeong, K. S., Lee, D. G., and Kwak, Y. K., *J. Adhesion* **48**, 195–216 (1995).
[6] Shin, K. C., and Lee, J. J., *J. Adhesion Sci. Tech.* **14**, 1691–1704 (2000).
[7] Choi, J. H., and Lee, D. G., *J. Compos. Mater.* **31**, 1381–1396 (1997).
[8] Lee, S. W., Lee, D. G., and Jeong, K. S., *J. Compos. Mater.* **31**, 2188–2201 (1997).
[9] Cho, D. H., Lee, D. G., and Choi, J. H., *Compos. Struct.* **38**, 309–319 (1997).

[10] Cho, D. H., and Lee, D. G., *J. Compos. Mater.* **32**, 1221–1241 (1998).
[11] Lee, D. G., and Cho, D. H., *J. Compos. Mater.* **34**, 689–722 (2000).
[12] Cho, D. H., and Lee, D. G., *J. Adhesion Sci. Tech.* **14**, 939–963 (2000).
[13] Shin, K. C., and Lee, J. J., *J. Adhesion Sci. Tech.* **16**, 347–359 (2002).
[14] Crane, L. W., Hamermesh, C. L., and Maus, L., *SAMPE J.* **12**, 6–9 (1976).
[15] Parker, B. M., and Waghorne, R. M., *Compos.* **13**, 280–288 (1982).
[16] Lee, D. G., Kim, K. S., and Im, Y. T., *J. Adhesion* **35**, 39–53 (1991).
[17] Wegman, R. F., *Surface Preparation Techniques for Adhesive Bonding* (Noyes Publications, Park Ridge, NJ, 1989), pp. 1–8.
[18] Renton, J. W., and Vinson, J. R., *Eng. Fract. Mech.* **7**, 41–60 (1975).
[19] Shin, K. C., Kim, Y. G., Lee, D. G., and Choi, J. M., *Compos. Struct.* **38**, 215–227 (1997).
[20] Choi, J. H., and Lee, D. G., *J. Compos. Mater.* **29**, 1181–1200 (1995).
[21] *Annual Book of ASTM Standards—General Products, Chemical Specialties, and End Use Products* (American Society for Testing and Materials, Philadelphia, PA, 1995), Vol. 15, pp. 240–243.
[22] *ABAQUS/Standard User's Manual* (Hibbit, Karlsson & Sorensen, Pawtucket, RI, 1998), Vol. 2, Chap. 14.1.4, pp. 1–17.
[23] Fontana, M. G., *Corrosion Engineering* (McGraw-Hill Book Company, Singapore, 1987), pp. 105–109.
[24] Burden, R. L., and Faires, J. D., *Numerical Analysis* (PWS-KENT Publishing Company, Boston, 1989), pp. 439–451.